



## An X-ray view of quasars

K. P. Singh<sup>1\*</sup>

<sup>1</sup>Tata Institute of Fundamental Research, Homi Bhabha Road, Mumbai 400 005, India

Received 2013 April 30; accepted 2013 June 03

**Abstract.** I present an overview of observational studies of quasars of all types, with particular emphasis on X-ray observational studies. The presentation is based on the most popularly accepted unified picture of quasars - collectively referred to as AGN (active galactic nuclei) in this review. Characteristics of X-ray spectra and X-ray variability obtained from various X-ray satellites over the last 5 decades have been presented and discussed. The contribution of AGN in understanding the cosmic X-ray background is discussed very briefly. Attempt has been made to provide up-to-date information; however, this is a vast subject and this presentation is not intended to be comprehensive.

*Keywords* : quasars: general – galaxies: active – galaxies: nuclei – galaxies: Seyfert – X-rays: galaxies – X-rays: diffuse background

### 1. Introduction

Quasars discovered about 50 years ago by astronomers working with radio and optical telescopes are the brightest sources of radiation in the sky over 20 decades of the electromagnetic spectrum from radio to  $\gamma$ -rays. These cosmic objects appear as point like or "quasi-stellar" on photographic plates and are so powerful that they emit nearly 5 to 8 orders of magnitude more radiation than the normal galaxies. Their emission is concentrated in a very small, nuclear region of what are now known as active galaxies. These also contain strong and broad optical emission lines. The somewhat lower luminosity analogs of these objects were in fact discovered two decades earlier by Carl Seyfert and these are known as the Seyfert galaxies. The optical emission from them is characterised by peculiar, broad, high ionization emission lines and these are believed to originate from the nuclear regions of these galaxies, with the total light output (continuum + lines)

---

\*email: Kulinderpal.Singh@tifr.res.in

exceeding the total light from the rest of the galaxies by 1 to 5 orders of magnitude. Such active galaxies make up about 1% of all galaxies. Even lower luminosity active galaxies (albeit more luminous than the normal galaxies) exist and are dubbed as LINERS (Low Ionisation Nuclear Emission Regions). LINERS are believed to be more numerous than the Seyfert types. All the different types of sources are collectively known as Active Galactic Nuclei and henceforth will generally be referred to as AGN, except while discussing some special properties.

Most of the AGN have very weak radio emission and are generally called Radio Quiet (RQ) quasars or RQ AGN or sometimes QSOs (Quasi Stellar Objects). About 10% of the optically bright quasi-stellar objects are strong radio sources. These powerful radio sources have been found to contain strong directed emissions, known as jets, and that is how these got the attention. It is this nature and their appearance in the optical that got them the name of "quasars" or Radio Loud (RL) AGN. There are several types of quasars known today depending on their observed characteristics in the optical. These are Blazars or BL Lac objects named after their highly variable prototype - BL Lac, FSRQs (Flat Spectrum Radio Quasars), HPQs (High Polarisation Quasars), and OVVs (Optically Violent Variables). See Peterson(1997), Kembhavi & Narlikar (1999), Krolik (1999) for comprehensive discussion of different AGN types.

X-ray emission from AGN is ubiquitous, and was discovered in the early rocket flights in the mid-sixties, just a few years after the discovery of quasars. High X-ray luminosity, comparable to that in the optical was detected in almost all of them. Very high luminosity is subject to Eddington limit which implies mass of greater than  $\sim 10^6 L_{44}$  solar masses, where  $L_{44}$  is luminosity in unit of  $10^{44}$  ergs  $s^{-1}$ . This combined with rapid variability, specially in X-rays, indicates that trillions of solar luminosities are generated in a region smaller than  $10^{13-15}$  cm. The powerful source in AGN is thus extremely compact and much more efficient than stellar processes. Accretion onto compact objects, which is known to be more efficient than nuclear fusion, is thus indicated. All these considerations suggest accretion onto a putative super massive black hole (SMBH) of mass in the range of a million to a billion solar masses as the primary source of energetic and powerful radiations from AGN. X-rays with their penetrative nature through large columns of gas and dust surrounding the SMBH are the most direct probe of the accretion processes responsible for this massive energy generation close to the SMBH.

AGN dominate the X-ray sky. Nearly 80% of all the X-ray sources in any medium-deep survey of the X-ray sky at high Galactic latitude are AGN, and are thus a major contributor to cosmic X-ray background that was largely unresolved until the early 1990s. These powerful AGN also have a significant impact on their environments and play a major role in process of galaxy formation via feedback through winds and ionisation of the interstellar media. New and unexpected populations are being discovered even now in the new and deeper X-ray surveys. In the local Universe, obscured AGN are seen to be more common than unobscured AGN by a factor of  $\sim 3-4$  (Risaliti et al. 1999). How does this ratio evolve at higher redshifts is an important question currently under study.

These heavily obscured AGN are also very important for the understanding of the cosmic X-ray background above a few keV, and are the targets of the studies of AGN in hard X-rays. Apart from solving the mystery of the cosmic X-ray background the new surveys are suggesting the existence of more than one major epoch of black hole mass accretion assembly in the history of the Universe.

In the following section (Section 2) I introduce the unified scheme of AGN structure (Fig. 1) and characteristics of different types of AGN. The unified scheme has been built up from multi-wavelength observations over the past few decades (Beckman & Shrader 2012). In Section 3, I briefly describe the various X-ray missions that have played, and are currently playing, a major role in the various milestones achieved in the study of AGN. Results obtained from X-ray spectral and timing measurements of AGN of various types are described in detail in Section 4. The role of the AGN in explaining the cosmic X-ray background is briefly described in Section 5, followed by a short discussion on the future directions in the study of AGN.

## 2. AGN structure: the unified scheme

The main physical components believed to exist in an AGN are displayed in the unified picture shown schematically in Fig. 1. The common powerhouse in each type of AGN is an accreting SMBH, while most of the differences amongst the various types can be ascribed to anisotropic AGN obscuring environments and their random orientations towards Earth (Fig. 1). The early ideas of unification in which orientation and relativistic motion may play an important role in the observed properties of AGN were suggested by Scheuer & Readhead (1979) in their attempt to unify radio-loud and radio-quiet quasars. These ideas were initially extended to lobe- and core-dominated radio loud quasars (Orr & Browne 1982; Kapahi & Saikia 1982) and later to radio-loud galaxies and quasars (Barthel 1989).

The idea of unification with an anisotropic AGN obscuring environment had its strongest evidence from spectro-polarimetric observations of the type 2 Seyfert NGC 1068 (Antonucci & Miller 1985), in which broad permitted lines generated close to the nucleus and usually seen in type 1 Seyferts were discovered through polarised light. It was suggested that in type 2 Seyferts an optically-thick obscuring matter (mostly dust) blocks the line-of-sight to the nucleus of NGC 1068, and thus the broad permitted lines are not seen directly. A small fraction of the radiation can, however, get scattered into our direction if the matter surrounding the AGN has a torus geometry. The scattered light is polarised, thus suggesting that the reflector consists of electrons in a plasma, presumably ionised by direct AGN radiation. The narrow-line region in all AGN lies above the torus and is irradiated by the photo-ionising continuum. Thus, the size and orientation angle of the torus to our line-of-sight is the key parameter that decides the appearance of an AGN. Broad permitted lines in type 2 AGN have also been discovered in the near-infrared by Goodrich et al. (1994), where the opacity is much lower than at optical wavelengths. The re-processed, warm, thermal radiation from the torus itself

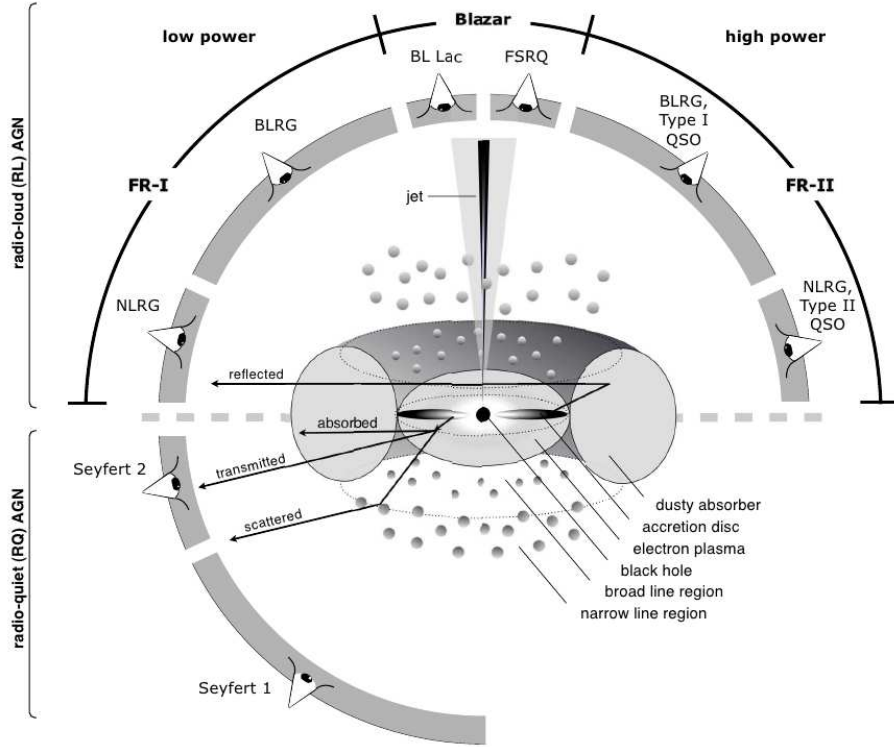


**Figure 1.** Schematic representation of our understanding of the AGN phenomenon in the unified scheme reproduced from Beckman & Shrader (2012) (By permission of the authors). The type of object we see depends on the viewing angle, the presence or the absence of the jet, and the power of the central engine in AGN. Note that radio loud objects are generally thought to display symmetric jet emission.

has been detected in the far-infrared (Wilman et al. 2000). It is the X-rays, however, that have the highest penetrating power through obscuring gas that is associated with the dusty torus surrounding the AGN.

Right at the centre of an AGN is an SMBH surrounding which is an accretion disk. The size of the accretion disk around an SMBH of  $10^6 M_{\odot}$  is of the order of light-days, which even at the distance of the nearest AGN, is too small to be resolved by the current generation of telescopes, since the resolution required is better than  $\sim 1$  milli-arcsecond. However, at radio frequencies it may be possible to image maser emission from the disk with high angular resolution using Very Long Baseline Interferometric techniques. For example, in the case of the AGN, NGC 4258, strong water maser emission has been used to map motions in the accretion disk (Miyoshi et al. 1995). Accretion disks in AGN are usually optically-thick and physically-thin (Shakura & Sunyaev 1973), and

have temperatures in the range of  $\sim 10^5 - 10^6$  K, making them sources of optical and ultraviolet radiation. This optical and UV continuum scatters off a corona of very hot electrons close to and above the accretion disk. The corona of electrons is probably heated by processes similar to the heating of the Solar corona, involving magnetic fields. Optical and UV photons from the disk undergo inverse-Compton scattering off hot electrons, and emerge as higher energy X-rays. Multiple scatterings within the corona boost the energy further, resulting in characteristic power-law non-thermal continuum extending from under 1 keV to several hundred keV. More details of the main features in AGN X-ray spectra are discussed in section 4.1.

The bulk of line emission from AGN, first used to classify the AGN, comes from discrete and patchy cloud-like structures much further out from the SMBH. These lines are generated mainly by photo-ionisation with some contribution from collisional excitation. The clouds closer to the SMBH have very broad permitted recombination lines (full width at half maximum: FWHM  $\sim 3000$  km s $^{-1}$  or more), and also have blue broad-band optical continua. Thus, a dense (electron density of  $10^7 - 10^{10}$  cm $^{-3}$ ) broad line region (BLR) is inferred to exist on scales smaller than a parsec (pc) within the deep gravitational potential of SMBH, leading to the large line-widths observed due to Doppler broadening. A technique called reverberation mapping that uses the delay time between continuum variation and subsequent emission line intensity variations suggests the size of this region to be  $0.1L_{46}^{0.5}$  pc (where  $L_{46}$  is the photoionising luminosity in units of  $10^{46}$  erg s $^{-1}$ ; Peterson 1993). The presence of BLR is responsible for designation of type 1 for the AGN. AGN where the narrow (FWHM  $\sim 500$  km s $^{-1}$ ) permitted lines dominate are designated type 2 AGN and usually possess red continua. Intermediate types also exist which display both narrow and broad components to the permitted lines. All types show significant forbidden lines, but these are always narrow, and thus suggesting the existence of a narrow line region (NLR), that extends over scales of tens to hundreds of pc, where the emitted lines are all narrow due to weaker gravity. The very existence of strong forbidden lines implies that densities in the NLR cannot exceed the critical density for collisional de-excitation, and are thus inferred to be low ( $\sim 10^4$  cm $^{-3}$ ) from analysis of various nebular line species such as the [OIII] 4959, 5007 Angstroms doublet. Temperatures of the photoionised media are difficult to ascertain due to dependence of radiative cooling on metallicity, but values of  $\sim 10^4$  K are typical for the NLR; the BLR being hotter by a factor of  $\sim 1.5 - 2$  (Osterbrock 1989).

In this unified scheme, quasars or Radio Loud (RL) AGN are objects with directed or relativistic jet emission which produces strong radio emission via Synchrotron process. Blazars are interpreted as a subset of these radio-sources where the relativistic jet is aligned almost along the line of sight (Urry & Padovani 1995). In other words, the class of blazars is represented by RL AGN observed very close to the direction of the relativistic jets ( $< 10^\circ$ ).

### 3. X-ray missions and some milestones in the studies of AGN

The first detections of X-rays from AGN were reported from 3C273 and M87 by Friedman & Byram (1967) in a survey of the Virgo region carried out using a proportional counter on an Aerobee rocket. They also suggested that combined contributions from such weak extragalactic sources could be responsible for the cosmic X-ray background already seen in the previous rocket flights. X-rays were subsequently detected from some Seyfert galaxies by the first dedicated X-ray satellite, Uhuru, launched in 1970 (Gursky et al. 1971). NASA's High Energy Astronomy Observatory (HEAO-1) launched in 1977, carried scintillation detectors in addition to proportional counters, and provided complete surveys of the X-ray sky, especially towards high Galactic latitude regions (Piccinotti et al. 1982). Apart from identifying and studying X-ray emission from AGN (Dower et al. 1980; Mushotzky et al. 1980) (and various other types of Galactic and extra-galactic objects) it also provided good spectral characterisation of the diffuse X-ray background radiation over the energy range 3 – 50 keV (Marshall et al. 1980). A simple power-law was found to characterise the X-ray emission from 3 to 50 keV. A soft X-ray bump in the power-law X-ray spectrum of a Seyfert was also first discovered with the low-energy detectors on board HEAO-1 (Singh et al. 1985). A veritable revolution in X-ray astronomy occurred when Einstein Observatory carrying the first X-ray telescope with focusing optics necessary to produce images (see Aschenbach (1985); Singh (2005, 2011) for an overview of X-ray imaging optics) was launched in 1978. Hundreds of extragalactic point-like X-ray sources, as well as diffuse and extended sources over 0.2 – 4 keV were imaged with superb spatial resolution of only a few arcsec. European Space Agency's EXOSAT and the Japanese Ginga satellites launched in the 1980s carried out much longer observations of some AGN. EXOSAT confirmed the existence of soft bumps in the X-ray spectra (Turner & Pounds 1989) and Ginga discovered the flattening of the hard X-ray spectra of AGN, indicating X-ray reflection (Pounds et al. 1990; Singh et al. 1990).

Another major advance in X-ray astronomy came with ROSAT, or Roentgen satellite in the soft ( $< 2$  keV) energy range. In an all-sky survey, with its large collecting area and high resolution optics, ROSAT detected  $>100,000$  X-ray sources (see Voges et al. 1999 and references therein). It was able to completely resolve the soft X-ray background into discrete sources (mostly AGN) through ultra-deep observations (Lehmann et al. 2001).

ASCA (Tanaka et al. 1994) and BeppoSAX (Boella et al. 1997) were important Japanese and Italian-led missions of the nineties respectively, that were responsible for detailed studies of AGN continua as well as Fe emission lines. ASCA with the first X-ray CCD camera in the focal plane of a light weight telescope was the first to find evidence for broad emission line from Fe fluorescence in a deep observation of an AGN (Tanaka et al. 1995), suggesting the broadening of the red-wing to be due to extreme gravitational field very close to the SMBH. X-ray flux variability at almost all time-scales from AGN was studied in detail by the dedicated satellite Rossi X-ray Timing Explorer (RXTE). RXTE, sensitive over the range 0.2 – 250 keV, made several important discoveries (see McHardy 2010 and Section 4.2).

Chandra X-ray Observatory with its unprecedented spatial resolution of  $\sim 0.5$  arcsec combined with its high sensitivity over the  $0.5 - 8$  keV range has led to the detection and identification of very faint X-ray sources. One of the main results from the mission has been the resolution of the cosmic X-ray background radiation (CXB) up to approximately 8 keV (Mushtozky et al. 2000). It is now recognised that the bulk of the CXB is the summed emission from a distribution of redshifted, and predominantly-obscured AGN. Two sets of X-ray transmission gratings that are present in the optical path of Chandra have been used to observe large numbers of emission and absorption lines from X-ray sources, including AGN. For instance, the spectrum obtained for the AGN at the centre of NGC 3783 shows hundreds of absorption features due to various ionic species of Fe, Mg, O, N, Ne, Si etc. (Kaspi et al. 2002). XMM-Newton, ESA's major X-ray observatory, complements Chandra by having a much larger collecting area (a factor of  $\sim 10$  larger at 2 keV) over  $0.3 - 10$  keV, but worse spatial resolution by a factor  $\sim 10$ . Due to its large collecting area and good spectral resolution, XMM-Newton is able to search for spectral features in distant cosmic sources fainter than those detectable by any previous mission: e.g., Fe emission lines in distant AGN.

The latest to join the array of X-ray Observatories is the Nuclear Spectroscopic Telescope Array (NuSTAR), launched in 2012 (Harrison et al. 2013). In the first result published using its ability to measure the high-energy ( $3 - 80$  keV) X-ray spectrum of NGC 1365 with unprecedented accuracy, Risaliti et al. (2013) report a clearer measurement of the broadening of the Fe fluorescence line that can be best explained as due to the spin (at least 84% of the maximum theoretically allowed value) of the SMBH in NGC 1365.

## 4. X-ray emission

### 4.1 X-ray spectra of radio-quiet AGN

The many prominent features seen in the X-ray spectra of radio-quiet type 1 AGN are shown in Figure 2 and discussed below:

(i) Power-law: AGN having a direct line-of-sight to the central black hole show a power-law continua over the  $0.5 - 10$  keV regime. These are usually parametrized in terms of photon density:  $N_E$  proportional to  $E^{-\Gamma}$  counts  $s^{-1} \text{ cm}^{-2} \text{ keV}^{-1}$ . In the local Universe, an average value of the photon-index  $\Gamma = 1.9$  is observed (Nandra & Pounds 1994), with typical range of  $1.7 - 2$ . The power-law usually attributed to non-thermal processes arises due to multiple up-scatterings of accretion disk photons undergoing inverse-Compton interactions off thermal hot electrons in the corona above the accretion disk.

(ii) Soft Excess: A soft emission component is often observed in AGN, with characteristic temperature  $kT \sim 0.2 - 1$  keV (Singh et al. 1985; Turner & Pounds 1989). The physical origin of this component is not clear: warm emitting gas could be located in the

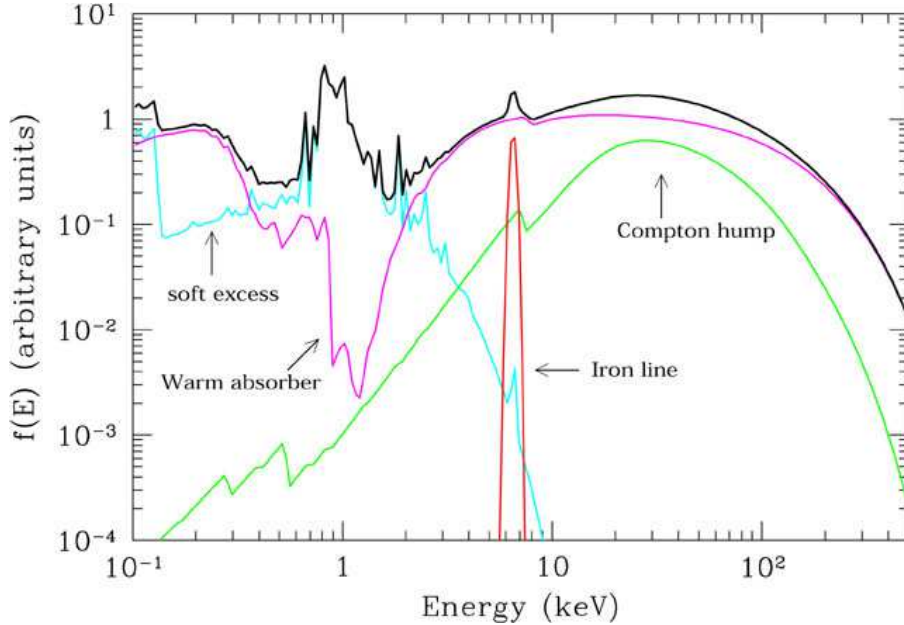


**Figure 2.** Average total spectrum (thick black line) and main components (thin grey lines) in the X-ray spectrum of a type I AGN. The main primary continuum component is a power law with a high energy cut-off at  $E \sim 100 - 300$  keV, absorbed at soft energies by warm gas with  $N_H \sim 10^{21} - 10^{23}$  cm $^{-2}$ . A cold reflection component is also shown. The most relevant narrow feature is the iron K emission line at 6.4 keV. Finally, a “soft excess” is shown, due to thermal emission of a Compton thin plasma with temperature  $kT \sim 0.1 - 1$  keV.

accretion disk, or in the broad line region (it could be the confining medium of the broad emission line clouds), or in a region farther from the centre. Alternatively, this “soft excess” could be an extension of the big blue bump to higher energies, e.g., via Compton scattering in a hot accretion disk corona (Czerny & Elvis 1987). AGN where the soft excess alone dominates the X-ray emission, have been discovered and are known as the Narrow Line Seyfert Type 1 (NLS1) galaxies since almost all of them have narrower permitted emission in the optical than seen in the regular Type 1 or broad line Seyferts. The power-law index of the X-ray emission from these objects is also found to be significantly steeper and inversely proportional to the width of the optical lines (Boller 1999). The steep power law could be the result of domination of X-ray reflection (see below) in the innermost regions of the accretion flow (Fabian et al. 2002). NLS1 show extreme (large amplitude) and rapid (short time scale) X-ray variability among all the Type 1 AGN.

(iii) Hard X-ray Bump and Reflection: A broad hump, or excess luminosity, is seen in many AGN over  $\sim 20 - 40$  keV above the canonical lower-energy power-law. This can be attributed to reflection of photons (George & Fabian 1991) briefly explained below:

The hard power-law that is seen directly also irradiates the accretion disk, which produces backscattered radiation, fluorescence, and recombination etc. This backscattered radiation or albedo is known as reflection. The reflection fraction depends on the ionisation state of the disk, but the overall effect is predicted to be a hardening or biasing of the spectrum towards higher energies, due to high albedo at 30 keV combined with photoelectric absorption of lower energy X-ray photons. A warm, ionized reflector must be present in the central region of many AGN (since we see a “warm absorber” in  $\sim 50\%$  of Seyfert 1 galaxies). The reflected emission has the same spectral shape as the incident continuum. For a review of X-ray reflection in AGN, see Fabian & Ross (2010) who also discuss how the reflection spectrum can be used to obtain the geometry of the accretion flow, particularly in the inner regions around SMBH.

(iv) Hard Cut-off: X-ray and  $\gamma$ -ray telescopes have discovered an exponential cut-off to the AGN power-law at energies between 100 – 300 keV. At these high energies (approaching the electron rest-mass energy of 512 keV), photons lose more energy than they gain in each Compton scattering because of electron recoil, resulting in a roll-over of the spectrum.

(v) Low Energy Absorption: Soft X-ray (below 10 keV) emission from AGN is usually absorbed or modified before it reaches the observer through photoelectric absorption. This is specially pronounced if the line-of-sight passes through the obscuring torus. A typical integrated line-of-sight obscuring column density that delineates the boundary between obscured and unobscured (Type 1 or Type 2 respectively) AGN is  $10^{22} \text{ cm}^{-2}$ . The absorbing column-density itself is parametrized in terms of Hydrogen atoms per  $\text{cm}^2$  integrated along the line-of-sight, though heavy elements such as O, Mg, Si, S and Fe are responsible for much of the opacity above 1 keV. Discrete photoelectric edges are observed at the ionisation energies for these heavy elements (Morrison & McCammon 1983). The obscuration associated with an e-folding decrease of transmitted radiation at 10 keV in the source rest-frame is  $\sim 1.5 \times 10^{24} \text{ cm}^{-2}$ , and these sources are called Compton-thick. Very little direct radiation is seen from these sources. Additionally, at very high column-densities, multiple scatterings, as modelled by the Klein-Nishina cross-section, lead to a Compton down-scattering over the full X-ray spectral regime, and very little direct flux emerges above column-densities larger than  $10^{25} \text{ cm}^{-2}$  (Wilman & Fabian 1999). The effect of varying absorption columns on the X-ray spectra of AGN is shown in Fig. 3 reproduced from Wilman & Fabian (1999).

(vi) Iron Emission line. The most prominent narrow feature in the 2 – 10 keV X-ray spectra of AGN is an iron emission line at energy 6.4 keV, corresponding to the  $\text{Fe-K}_{\alpha} = 2 - 1$  transition of “cold” (i.e., Fe I – FeXVII) iron. The typical EW of the line is observed to be 100 – 200 eV. The line is usually ascribed to emission due to fluorescence in the inner part of the accretion disk. The rotation of the accretion disk leads to the doppler-splitting of the line on the approaching and receding sides of the disk relative to the observer; line photons lose energy due to strong gravitational redshift as the photons climb out of the deep potential well associated with the central BH; further distortion

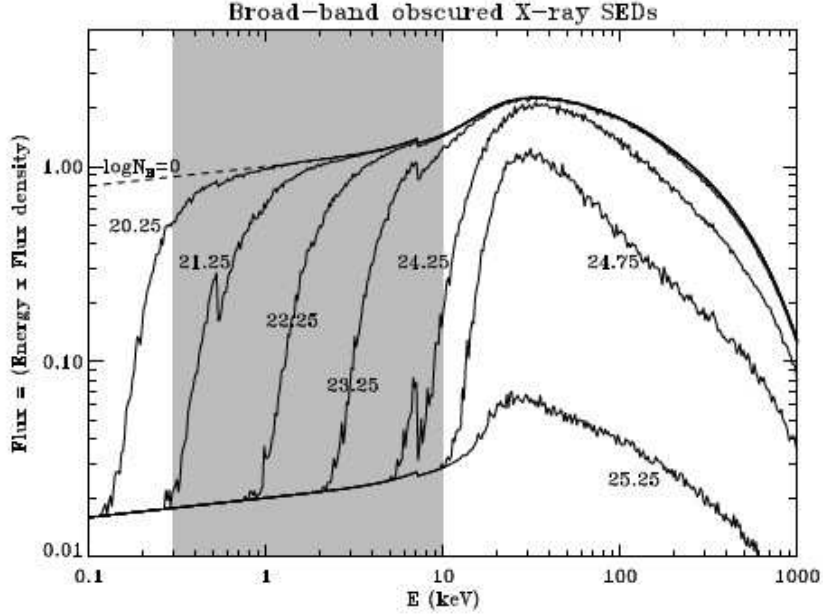


**Figure 3.** Rest-frame X-ray spectral energy distributions (SEDs) showing the effect of absorption by material of solar abundance local to the source. Absorbers assumed have column densities  $\log(NH)$  ranging from 20.25 to 25.25. Cross-sections used are from Morrison & McCammon (1983), and Compton down-scattering is modelled with the full Klein-Nishina cross-section. The continuum spectra were modelled with intrinsic AGN power-law with photon-index  $\Gamma=1.9$  and include a reflection hump from cold material at solar abundance assuming uniform  $2\pi$  reflection and an inclination angle of 60 degrees, as well as an exponential cut-off at 360 keV. Two percent of the primary radiation is added to each SED to model the scattered component into the line-of-sight. See Wilman & Fabian (1999) for details. The shaded region marks the X-ray spectral regime accessible to Chandra and XMM-Newton. Courtesy: Wilman & Fabian (1999).

occurs due to relativistic boosting of the blue (approaching) part of the spectrum relative to the red part and due to the transverse doppler effect associated with time dilation. The net, predicted line profile has a blue peak and a hump with an extended red tail (see Fig. 4), each feature being sensitive to BH characteristics such as mass, spin etc. Asymmetric profiles have been calculated for lines emitted at a few Schwarzschild radii from non-rotating (George & Fabian 1991; Fabian & Ross 2010) and rotating (Laor 1991) black holes. Evidence for a broad “red wing” extending to lower energies was first detected with ASCA (Tanaka et al. 1995). Once thought to be widespread, XMM-Newton spectra of the red wing have been clearly seen only in a few objects e.g., MCG-6-30-15 (Vaughan & Fabian 2004), 1H0707-495 (Fabian et al. 2009; Fig. 4). Most recently, broad-band X-ray (3 - 79 keV) observations of a low luminosity Seyfert NGC 1365 with NuStar reveal the relativistic disk features through an asymmetrically broadened Fe-line emission and

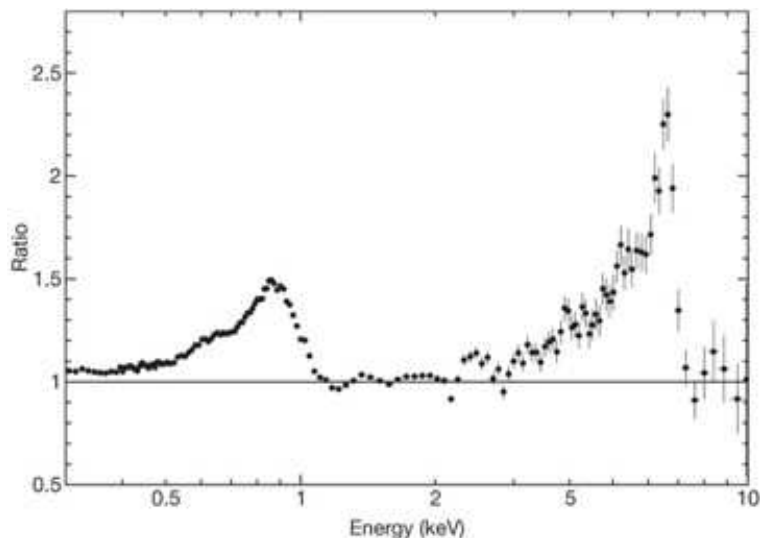


**Figure 4.** Ratio of the observed XMM-Newton spectrum of 1H0707-495 and a model consisting of a power law, a black body and two broad emission lines, where the normalizations of the broad lines have been set to zero to make the plot. Ionised Fe L and K emissions peaking in the rest frame around 0.9 keV and 6.5–6.7 keV with equivalent widths of 180 and 970 eV, respectively, can be seen. Error bars are  $1\sigma$ . Courtesy: Fabian et al. (2009).

an associated Compton scattering excess of 10–30 keV (Risaliti et al. 2013). Using temporal and spectral analyses, Risaliti et al. disentangled the continuum changes due to time-variable absorption from reflection, which appears to arise from a region within 2.5 gravitational radii of a rapidly spinning black hole in NGC 1365.

A second, narrow component of the Fe-K line is also present in most AGN. The width of this “narrow” line (which is unresolved in CCD spectra from ASCA, Chandra ACIS, or XMM-Newton EPIC) is a few  $1000 \text{ km s}^{-1}$  or smaller when measured with the high energy transmission grating (HETG) spectrograph of Chandra. This is similar to the width of optical and UV broad emission lines. This narrow component does not vary when the continuum varies, even for delay times of days. Coupled with the line width, this suggests an origin well beyond a few Schwarzschild radii, although a smaller radius is not fully ruled out (Fabian et al. 2002). If the reflector is highly ionised, the peak energy of this line can be shifted toward high energies (6.7 keV for helium-like iron and 6.96 keV for hydrogen-like iron). It is also possible that two narrow components are present in the spectrum, one emitted by a cold reflector and the other by an ionised reflector. CCD detectors like the ASCA SIS or XMM-Newton EPIC (with energy resolution of  $\sim 120 - 150 \text{ eV}$  at 6 keV) are unable to separate these two lines, while the Chandra HETG spectrograph has limited effective area ( $\sim 40 \text{ cm}^2$ ) at 6 keV.



location and size of the X-ray source in AGN. The first detailed observations of AGN X-ray variability were made by EXOSAT (Lawrence et al. 1987). However, it was with RXTE observations in the last  $\sim 16$  years that a detailed picture has emerged and the reader is referred to McHardy (2010) where the author also compares the AGN with black-hole binary systems (BHBs) in the Galaxy. On long time scales of months to years, BHBs are found to be in the hard, or soft or VHS (Very High State) states. In the hard state the medium energy X-ray flux is low and the spectrum is hard. In the soft state, the medium energy X-ray flux is high and the spectrum soft, whereas in the VHS the spectrum is intermediate in hardness between the hard and soft states. Type I AGN, on the other hand are usually found to have X-ray spectra that are similar to those of hard state BHBs (i.e. photon indices  $\sim 2$ ), and much harder than soft state BHBs.

#### 4.2.1 Power spectral distributions and time lags between hard and soft X-rays

The X-ray timing properties of the different spectral states are characteristically different and may provide a better discriminant of the ‘states’ than the spectral properties. X-ray variability is usually quantified in terms of the power spectral density (PSD) of the X-ray light curve. The PSD of BHBs have a power-law spectrum  $P(\nu) \propto \nu^{-\alpha}$  with a bend at high frequencies (slope,  $\alpha$ , goes from 2 to 1) in all their spectral states. In the hard state, the PSD shows an additional bend at low frequencies ( $\alpha$  going from 2 to 0). The frequency at which the bends occur refer to characteristic time scale of the systems defined by the mass of the black hole and their accretion rate or ratio of luminosity to the the Eddington luminosity. Measuring the PSDs of AGN are, however, difficult because it requires encompassing a wide enough frequency range to detect the equivalent of the bends seen in PSDs of BHBs and the data are irregularly sampled. Assuming to first order that system sizes, and hence most relevant timescales, will scale with black hole mass,  $M_{BH}$ , then as the break frequency  $\nu_B$  is  $\sim 10$ Hz for the BHB Cyg X-1 in the high state [ $M_{BH} \sim 10-20M_{\odot}$ ], the expected  $\nu_B$  would  $\sim 10^{-7}$  Hz for an AGN with  $M_{BH} = 10^8 M_{\odot}$ . To measure such a bend requires a light curve stretching over a number of years. Uttley et al. (2002) describe a method that is used to derive PSDs from irregularly sampled light curves. Using this method for several AGN detects only one bend, from  $\alpha=2$  at high frequencies to  $\alpha=1$  at lower frequencies thus suggesting that only a soft state PSD is present in AGN (McHardy 2010) and is consistent with AGN being very bright due to moderate to high accretion rates. A couple of AGN, like Akn 564 and Ton S 180, appear to be accreting at nearly the Eddington rate and believed to be always in the VHS. The PSD of these objects also show double bends but these are better described as two Lorentzians (McHardy et al. 2007; McHardy 2010).

Study of time lags between soft and hard X-ray light curves is another useful diagnostic to understand the physical processes in AGN. Vaughan & Nowak (1997) and Nowak et al. (1999) describe a statistic, the coherence function, that is derivable from the cross spectrum used to compute phase or time lags between two time series e.g., soft and hard X-ray light curves, as a function of frequency. Applying this method to Akn 564 and Ton

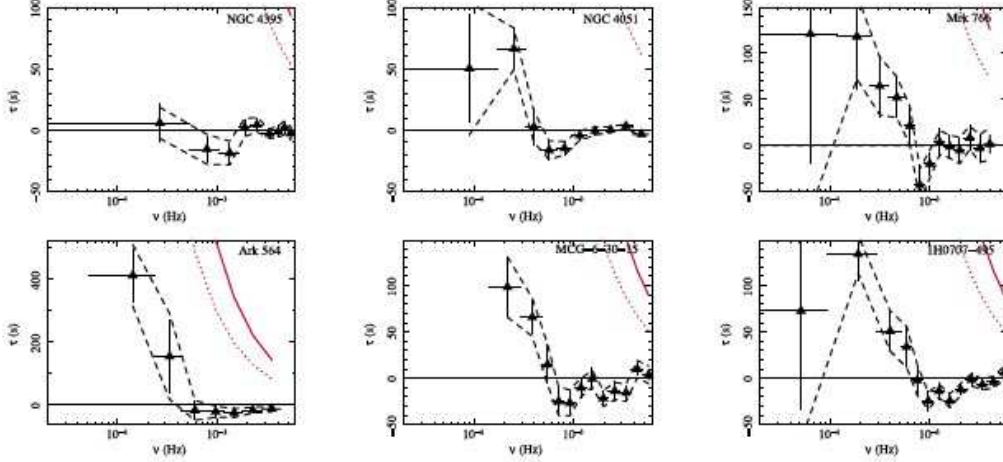


**Figure 6.** Hard and soft X-ray Lag–Frequency spectra of 6 the 32 sources reported by de Marco et al. (2013). Detected soft/negative lag at  $2\sigma$  confidence level are shown. The error bars are calculated as shown in Nowak et al. (1999). For further details see De Marco et al. (2013). Courtesy: de Marco et al. (2013)

S 180 showed that the nature of the lag changes with frequency and this frequency is related to the transition point from one Lorentzian to another. In Akn 564, a positive lag of  $\sim 600$ s of hard X-rays for frequencies lower than  $0.0004$ Hz changes to a negative lag of  $-11 \pm 4.3$ s at higher frequencies i.e., at high frequencies the soft X-rays lag the hard X-rays (McHardy et al. 2007; McHardy 2010; De Marco et al. 2013 and references therein). The hard lags are usually explained as due to multiple Compton scatterings of the low energy seed photons from the accretion disk to higher energies by a surrounding corona of very hot electrons. The soft lag would imply that in the very innermost part of the accretion disk corresponding to high frequencies in the coherence spectrum, the soft X-rays originate mainly from reprocessing of harder X-rays by the accretion disk.

#### 4.2.2 Reverberation mapping and lags between reflected and direct X-rays

The decomposition of the spectrum into direct and reflected emission components can be used in interpreting the reverberation lag as a signature of the light travel time between the corona (the hard X-ray continuum source) and the accretion disk (which reprocesses the flux into a reflection component with atomic spectral features like the Fe- $K\alpha$  line). Recently, a time delay of a few kilo-seconds was measured between the 2–3 keV band of the direct emission and the peak of the Fe  $K\alpha$  line in NGC 4151 (Zoghbi et al. 2012). The change of lag with energy resembles the shape of an iron  $K\alpha$  line broadened by relativistic effects. In addition, the line has a stronger blue horn at long timescales and a prominent red wing at short timescales, in a striking match to the expectation of a line

emitted from a disk and distorted by relativistic effects (Fabian & Ross 2010). Detection of Fe K lags has also been seen in 1H0707-495, IRAS 13224-3809, MCG-5-23-16 and NGC 7314 (Kara et al. 2013; Zoghbi et al. 2013). In the last two objects, the 6–7 keV band, where the Fe K $\alpha$  line peaks, lags the bands at lower and higher energies with a time delay of  $\sim 1000$ s. These lags are fully consistent with reverberation of the relativistically broadened iron K $\alpha$  line. The measured lags, their time scale, and spectral modelling indicate that most of the radiation is emitted at  $\sim 5$  and 24 gravitational radii for MCG-5-23-16 and NGC 7314, respectively (Zoghbi et al. 2013).

At luminosities  $L \geq 10^{-2} L_{Edd}$ , observations of Seyfert AGN show the clear presence of a more compact X-ray emitting source (the corona; e.g. McHardy et al. 2006) on top of a geometrically-thin, optically thick accretion disk extending as far in as the radius of the innermost stable circular orbit (ISCO). At lower luminosities, the hard X-rays most likely come for a much larger region. Due to the scale-invariant nature of the physics governing accretion flows onto BHs, the lag time scale depends primarily on the mass of the central BH:  $t \sim GM/c^3 = r_g/c$ , where  $r_g$  is the Schwarzschild radius for an SMBH of mass  $M$ . Reis & Miller (2013) estimate the probability distribution for the distances between the coronae and accretion disks by drawing samples from the probability distribution of the lag times and masses and apply to a sample of 17 radio-quiet Seyferts with luminosities  $\geq 10^{-2} L_{Edd}$  for which soft lags have been measured. They show that 14 out of 17 sources in their sample are indeed very compact and at distances strongly clustered around  $2-3r_g$  above the accretion disk or less than  $10r_g$  for all the sources even when the systematic uncertainties are taken into account. According to them, coronal models wherein most of the hard X-ray emission derives from magnetic reconnection in the innermost disk and/or from processes in the compact base of a central, relativistic jet are favoured.

### 4.3 Broad Absorption Line quasars (BALQSOs)

Some quasars show Broad Absorption Lines or BALs in their optical and UV spectra. The lines are almost saturated and blue-shifted with outflow velocities as large as  $0.1c$  (Weymann & Morris 1991). These troughs can be as wide as  $2000 - 20000 \text{ km s}^{-1}$  and are due to resonance absorption in the gas. About 10% of QSOs exhibit BAL troughs, but this is usually attributed to an orientation effect. No broad emission lines are observed with comparable widths, implying that the covering factor of the BAL region must be  $< 20\%$  (Hamann et al. 1993). This observation, together with the fraction of quasars showing BALs suggests that most or possibly all quasars contain BAL-type outflows. Indeed, counting weaker absorption systems, such as mini-BALs, narrow absorption lines, and associated absorptions, the fraction of AGN with outflows is at least 40%-60% (Dai et al. 2008). BALQSOs may thus provide a unique probe of conditions near the nucleus of most QSOs. In the orientation scenario, we expect that the intrinsic X-ray emission of BALQSOs should be similar to that of normal quasars. Therefore, an understanding of BAL outflows is required for an understanding of quasars as a whole.

X-ray spectroscopy of BALQSOs is important to study the properties and dynamics of absorbing outflows. This has, however, been difficult since BALQSOs are faint X-ray sources. One of the first attempts to study a BALQSO in X-rays with a wide field of view detector onboard EXOSAT and ASCA indicated heavy absorption in PHL5200 (Singh et al. 1987; Mathur et al. 1995), but was confused with another very faint quasar very close to PHL5200. Subsequently, ROSAT observations with a finer point spread function revealed that BALQSOs as a class are quiet in soft X-rays, and have unusually steep optical-to-X-ray slopes,  $\alpha_{ox} \geq 1.94$  relative to non-BAL QSOs  $\alpha_{ox} \sim 1.6$ ). Polarization studies also imply high column density absorption along the line of sight (Goodrich 1997). It is now believed that the BAL material has an absorbing column at least an order of magnitude larger than that estimated from UV spectra alone. ASCA observations (Gallagher et al. 1999) pushed up the column density lower limit by an order of magnitude above the ROSAT value. The absorbing columns in some cases are at least  $5 \times 10^{23}$ , within a factor of three of being Compton thick. Deep (100 ks) ASCA observations of an optically bright BALQSO ruled out the possibility of BALQSOs being intrinsically X-ray weak, instead strong absorption was clearly indicated (Mathur et al. 2000). The sharp point-spread function of Chandra enabled easy detections of the high-ionization BALQSOs (Green et al. 2001). The low-ionization BALQSOs, however, were found to be significantly more X-ray weak, implying either much larger absorbing column densities or intrinsically different X-ray characteristics. The XMM spectroscopy confirmed that high-ionization BALQSOs are highly absorbed in X-rays, but the nature of their continuum shape remained unresolved (Grupe et al. 2003). No other property of BALQSOs, including radio-loudness and polarization fraction, was found to correlate with X-ray brightness (Gallagher et al. 2006). Almost all X-ray data of BALQSOs are consistent with continuum spectral slopes similar to normal quasars, but steeper slopes were not ruled out in most cases. A steep slope is implied in the case of the  $z = 5.8$  BALQSO SDSS1044-0125 (Mathur 2001). All authors, however, agree on one important result: that strong X-ray absorption is a defining characteristic of BALQSOs.

BALQSOs were thought to be only radio quiet; however, radio-loud BALQSOs have been discovered with sensitive radio surveys (Becker et al. 1997). The fraction of BALs decreases with increasing radio luminosity (Shankar et al. 2008), partially explaining the initial failures when searching for BALs in radio-loud quasars. Schaefer et al. (2004) found that XMM-Newton spectrum of radio-loud BALQSOs showed it to be brighter than the radio-quiet BAL quasars and having a partial covering X-ray absorber. This implies that even radio-loud BALQSOs exhibit some soft-X-ray absorption as do radio-quiet BALQSOs. Miller et al. (2009), based on Chandra observations of BALQSOs, (note that these studies are based on X-ray detections with counts too few to perform spectroscopy) find that radio-loud BALQSOs are X-ray weak relative to their non-BAL counterparts. Miller et al. also note that while some radio-loud BALQSOs have harder X-ray spectra than typical radio-loud quasars, some do not.

#### 4.4 Radio loud AGN: quasars and blazars

Radio-loud AGN: quasars and blazars, are very strong emitters of radiation at almost all the wavelengths: radio, mm, infra-red, optical, ultra-violet, X-ray and  $\gamma$ -rays from MeV to TeV. The Spectral Energy Distribution (SED) of blazars, usually shows two broad-band humps which are usually believed to be produced via synchrotron (peaking in the infra-red to soft X-ray energy band) and Inverse Compton (IC) emission, dominating the hard X-ray to gamma-ray regimes, respectively. The lower energy (radio-to soft X-rays) emission component is synchrotron radiation from the jet whereas the high-energy component is believed to arise through the inverse-Compton scattering of soft photons by highly relativistic electrons in the jet plasma. These soft photons could originate from the local synchrotron radiation within the jet producing the Synchrotron Self-Compton (SSC) component or they could originate from the nuclear IR/optical/UV emission producing the External Compton (EC) component (see Maraschi, Ghisellini & Celotti 1992; Dermer & Schlickeiser 1993; Sikora, Begelman & Rees 1994).

The X-ray spectrum of a RL AGN is usually well described by a power-law with a specific flux (i.e., per unit energy interval) of the form  $N(E) \propto E^{-\Gamma}$ , where  $E$  is the energy,  $N(E)$  is the number of photons in units of  $s^{-1} \text{ cm}^{-2} \text{ keV}^{-1}$  and  $\Gamma$  is the photon index. X-ray spectra of blazars, however, show some deviations from the simple power-law. These spectral signatures appear in the soft X-ray band with a curvature (a flattening or a steepening of the spectrum). Two physical interpretations for the flattening of the primary intrinsic continuum with respect to a simple power-law exist (Page et al. 2005; Galbiati et al. 2005; Yuan et al. 2006). These are: (i) absorption in excess of the Galactic component (e.g. Cappi et al. 1997; Yuan et al. 2006), and (ii) a break in the intrinsic continuum (Sikora, Begelman & Rees 1994; Tavecchio et al. 2007). For the absorption excess, a dependence between the hydrogen column density of the absorber ( $N_H$ ) and the redshift  $z$  has been proposed. In fact in a former work by Yuan et al. (2006) based on XMM observations of a sample of 32 RL sources, a  $N_H$ - $z$  correlation has been found. Supporting evidence and a confirmation for the existence of this correlation has been provided by Gianni et al. (2011) who reported higher absorption at  $z > 2$  for a larger sample compared to the previous results. Gianni et al. used broad-band (0.2 – 100 keV) X-ray data obtained from Suzaku, Swift and INTEGRAL and also presented the distribution of the  $N_H$  and the photon index  $\Gamma$ . The hard X-ray data allowed them to detect highly absorbed sources (with  $N_H \geq 10^{23} \text{ cm}^{-2}$  in the rest-frame of the source). They also found that for these sources the photon index distribution peaked at harder values ( $\Gamma \sim 1.4$ ) with respect to that obtained with XMM data only ( $\Gamma \sim 2$ ).

In addition, and contrary to radio quiet (RQ) AGN, the presence of reflection features - most notably the Fe  $K_\alpha$  line and the associated Compton reflection hump at about 20 – 30 keV from the cores of the RL AGN is not well established. In RL AGN the iron line and the reflection component can be absent or weak. Some of the RL AGN, known as Broad Line Radio Galaxies, however seem to show weak hard X-ray reflection features in observations with ASCA, RXTE and Beppo SAX (e.g. Sambruna, Eracleous & Mushotzky

1999; Eracleous, Sambruna & Mushotzky 2000; Grandi et al. 2001; Ballantyne, Ross & Fabian 2002; Grandi & Palumbo 2004; Grandi, Malaguti & Fiacchi 2006).

#### 4.4.1 *X-ray variability of quasars and blazars*

X-ray observations of many quasars and blazars reveal very high variability on various time scales - from flares on minutes to hours to secular changes over days and years. McHardy (2010) have analysed X-ray data of 3C273, one of the most powerful quasars with a jet, collected from a large number of satellites over several years. They show that the PSD of 3C273 is exactly like that of a soft state Seyfert galaxy implying that the source of the variations – “note, not the source of the X-rays” – lies outside the jet and is simply modulating the emission from the jet e.g., variations propagating inwards through the disc. The jet then would be seen as an extension of the corona which dominates the emission in Seyfert galaxies (McHardy 2010).

The flares in blazars show a rich and complex behavior. The first observations which were detailed enough to show time structure in various energy bands (Takahashi et al. 1996) revealed that the soft X-rays lagged behind the hard ones in Mrk 421. This was explained as due to synchrotron cooling, i.e., lower energy electrons cool at a slower rate than the higher energy ones, and thereby explaining why the soft X-rays appear after the harder ones. Subsequent observations, however, showed cases of the opposite trend (Takahashi et al. 2000). This was attributed to particle acceleration since synchrotron cooling could not explain this. As fresh particles are accelerated to high energies, they radiate first soft and later hard photons, i.e. hard X-rays lag soft X-rays. Long, uninterrupted observations (Brinkmann et al. 2005) revealed that Mrk 421 shows both kinds of lags, with typical timescales of the order of 103s. The same mixed behavior was also verified for the same source by Tramacere et al. (2009). Finally, blazar 1ES 1218+304 showed a hard lag during a giant flare (Sato et al. 2008). Moraitis & Mastichiadis (2011) using two-zone acceleration model show that the best way to explain its flaring behavior is by varying the rate of particles injected in the acceleration zone. Their model is capable of producing a variety of flaring patterns despite the assumption of synchrotron losses dominating the energy loss mechanism, and ignoring the inverse Compton scattering as a possible electron energy loss mechanism. This can be justified for sources where the energy density due to magnetic fields exceeds the one due to photons.

## 5. Cosmic X-Ray background and heavily absorbed AGN

Discovered two years before the better-known microwave background (Giacconi 1962) cosmic X-ray background (CXB) covers a very wide energy range, extending from  $\sim 0.1$  keV to several hundred keV. In the very soft X-ray band ( $\leq 0.30$  keV), more than 90% of the CXB likely originates as thermal emission in a local bubble of hot, optically-thin ( $\sim 10^6$  K) gas in the solar neighbourhood (Singh et al. 1983). Between 2–10 keV, a

power-law with a photon-index  $\Gamma = 1.4$  [ $N(E) = E^{-\Gamma}$ ] was usually found to fit the data. HEAO-1 provided a more precise measurement of the spectrum of the CXB over the range 3–50 keV showed that it can be fitted to a diffuse 40 keV thermal bremsstrahlung model (Marshall et al. 1980). It also found that at these energies the CXB is isotropic to within a few per cent on large scales, after account is taken of a weak Galactic component as well as the dipole radiation field due to the motion of our Galaxy. However, its origin in the diffuse hot intergalactic medium is no longer supported and recent observations with XMM-Newton and Chandra have shown that the integrated emission from a wide distribution of AGN at various redshifts and with different obscuring column densities can account for the bulk of the CXB. The highly perceptive observation made by Friedmann & Byram with regard to CXB way back in 1967, has thus been proven to be correct for the energy range of 2–10 keV, even though uncertainty of  $\sim 30\%$  remains on the exact normalisation of the X-ray background intensity due to cross-calibration difficulties between various satellite missions, at least 75% of the CXB between 2–10 keV is now resolved (Mushotzky 2000). A significant percentage of CXB still unaccounted for, if one considers only 10–50 keV energy band (Worsley et al., 2004), and this could arise from truly diffuse emission or be due to distant and unresolved heavily obscured / Compton-thick AGN (Frontera et al. 2007) as their spectra can mimic the residual spectrum of the CXB. Indeed a large numbers of so-called type-2 QSOs, or AGN with intrinsic luminosities similar to those of local population, but hidden behind large obscuring columns of  $\log(NH) = 22$  or higher are being discovered with X-ray satellites (Gandhi et al. 2004; Zakamska et al. 2004.) X-ray bright optically normal galaxies (XBONGs: see Comastri et al. 2002; Miolino et al. 2003) found in luminous, as well as faint, X-ray sources, possibly constituting  $\sim 10\%$  of all X-ray selected AGN may be the other significant contributors to the hard X-ray CXB. Heavily absorbed AGN may outnumber their unobscured counterparts by a large factor, and it is likely that their numbers may have been underestimated because of the difficulty of detecting and identifying them.

## 6. Future

Multi wavelength studies of existing well known AGN, as well as distant and faint populations of AGN being discovered, are continuing to reveal a variety of activities in AGN, both in the spectral nature of these objects as well as the variability characteristics across the wavebands from simultaneous studies. This is making the overall picture more complex at the same time revealing a lot of information required to understand not only their violent activity but also about their life-cycles. How do the SMBH in AGN grow? What is the symbiosis of growth between the SMBH and their hosts? Does their life-cycle follow a monotonic path of growth or does it evolve through stages of quiet and resurgent periods? The expected launch of future X-ray missions like ASTRO-H and ASTROSAT, and the expected new generation of extremely large optical telescopes might have an important impact on understanding the physics of the multifrequency behaviour of AGN.

## References

- Antonucci R. R. J., Miller J. S., 1985, *ApJ*, 297, 621  
 Aschenbach B., 1985, *Rep. Prog. Phys.*, 48, 579  
 Ballantyne D. R., Ross R. R., Fabian A. C., 2002, *MNRAS*, 332, L45  
 Barthel P.D., 1989, *ApJ*, 336, 606  
 Becker R. et al., 1997, *ApJ*, 479, L93  
 Beckmann V., Shrader C.R., 2012, *Active Galactic Nuclei*, Wiley-VCH Verlag GmbH  
 Boella G., Butler R. C., Perola G. C., Piro L., Scarsi L., Bleeker J.A.M., 1997, *A&AS*, 122, 299  
 Boller, Th., 1999, *AIP Conf. Proc.: X-RAY ASTRONOMY: Stellar Endpoints, AGN, and the Diffuse X-ray Background*, **599**, 25.  
 Brinkmann, W., Papadakis, I. E., Raeth, C., Mimica, P., & Haberl, F. 2005, *A & A*, **443**, 397.  
 Cappi, M., Matsuoka, M., Comastri, A. et al., 1997, *ApJ*, **478**, 492.  
 Comastri A. et al., 2002, *ApJ*, 571, 771  
 Czerny B., Elvis M., 1987, *ApJ*, 321, 305  
 Dai X., Shankar F., Sivakoff G. R., 2008, *ApJ*, 672, 108  
 De Marco B., Ponti G., Cappi M., Dadina M., Uttley P., Cackett E. M., Fabian A. C., Miniutti G., 2013, *MNRAS*, 431, 2441  
 Dermer C. D., Schlickeiser R., 1993, *ApJ*, 416, 458  
 Dower R. G., Bradt H. V., Doxsey R. E., Johnston M. D., Griffiths R. E., 1980, *ApJ*, 235, 355  
 Eracleous M., Sambruna R., Mushotzky R. F., 2000, *ApJ*, 537, 654  
 Fabian, A.C. et al., 2002, *MNRAS*, 335, L1  
 Fabian A. C., Ballantyne D. R., Merloni A., Vaughan S., Iwasawa K., Boller Th., 2002, *MNRAS*, 335, L35  
 Fabian A. C. et al., 2009, *Nature*, 459, 540  
 Fabian A.C., Ross R. R., 2010, *Sp. Sci. Rev.*, 157, 167  
 Friedman H., Byram E. T., 1967, *Science*, 158, 257  
 Frontera F., et al., 2007, *ApJ*, 666, 86  
 Galbiati, E., Caccianiga, A., Maccacaro, T. et al., 2005, *A & A*, **430**, 927.  
 Gallagher, S. C., Brandt, W. N., Sambruna, R. M., Mathur, S., Yamasaki, N., 1999, *ApJ*, **519**, 549.  
 Gallagher, S. et al. 2006, *ApJ*, **644**, 709.  
 Gandhi, P., Crawford, C. S., Fabian, A. C., Johnstone, R. M., *MNRAS*, **348**, 529.  
 George, I. M. and Fabian, A. C., 1991, *MNRAS*, **249**, 352.  
 Giacconi R., 1962, *Phy. Rev. Letts.*, 9, 439  
 Gianni S., de Rosa A., Bassani L., Bazzano A., Dean T., Ubertini P., 2011, *MNRAS*, 411, 2137  
 Goodrich, R. W., Veilleux, S., and Hill, G. J., 1994, *ApJ*, **422**, 521.  
 Goodrich, R. 1997, *ApJ*, **474**, 606.  
 Grandi, P., Maraschi, L., Urry, C. M. & Matt G., 2001, *ApJ*, **556**, 35.  
 Grandi, P. & Palumbo, G. C., 2004, *Science*, **306**, 998.  
 Grandi, P., Malaguti, G. & Focchi, M., 2006, *ApJ*, **642**, 113.  
 Green, P. et al. 2001, *ApJ*, **558**, 109.  
 Grupe, D., Mathur, S., & Elvis, M. 2003, *AJ*, **126**, 1159.  
 Gursky, H., Kellogg, E. M., Leong, C., Tananbaum, H., and Giacconi, R., 1971, *ApJ. Letters*, **165**, L43.  
 Hamann, F. et al. 1993, *ApJ*, **415**, 541.  
 Harrison, F., et al. 2013, *ApJ*, in press *astro-ph arXiv:1301.7307v1*  
 Kapahi V.K., Saikia D.J., 1982, *JA&A*, 3, 465

- Kara, E., Fabian, A. C., Cackett, E. M., et al. 2013, *MNRAS*, **428**, 2795
- Kaspi, S. et al., 2002, *ApJ*, **574**, 643.
- Kembhavi A. K., Narlikar J. V., 1999, Quasars and active galactic nuclei: An introduction, Cambridge University Press
- Krolik, J. H., 1999, *Active galactic nuclei : from the central black hole to the galactic environment*, Princeton University Press.
- Krongold, Y., Nicastro, F., Brickhouse, N. S., Elvis, M., Liedahl, D. A., & Mathur, S. 2003, *ApJ*, **597**, 832
- Laor A., 1991, *ApJ*, 376, 90
- Lawrence, A., Watson, M. G., Pounds, K.A., et al., 1987, *Nature*, **325**, 694.
- Lehmann, I. et al., 2001, *A&A*, **371**, 833.
- Maiolino, R. et al., 2003, *MNRAS*, **344**, L59.
- Maraschi, L., Ghisellini, G., and Celotti, A., 1992, *ApJ Letters*, **397**, L5.
- Marshall, F. E. et al., 1980, *ApJ*, **235**, 4.
- Mathur, S., Elvis, M., Singh, K. P. 1995, *ApJ Letters*, **455**, L9.
- Mathur, S. 2000, *MNRAS*, **314**, L17.
- Mathur, S. 2001, *AJ*, **122**, 1688.
- McHardy I. M., Koerding E., Knigge C., Uttley P., Fender R. P., 2006, *Nature*, **444**, 730.
- McHardy, I. M., Ar?evalo, P., Uttley, P. et al., 2007, *MNRAS*, **382**, 985.
- McHardy, I. M., 2010, *The Jet Paradigm, Lecture Notes in Physics; Springer-Verlag Berlin Heidelberg*, **794**, 203.
- Miller, B. P. et al. 2009, *ApJ*, **702**, 901.
- Miyoshi, M. et al., 1995, *Nature*, **373**, 127.
- Moraitis, K., & Mastichiadis, A., 2011, *A & A*, **525**, 40.
- Morrison, R., McCammon, D., 1983, *ApJ*, **270**, 119.
- Mushotzky, R. F., Marshall, F. E., Boldt, E. A., Holt, S. S., Serlemitsos, P. J., 1980, *ApJ*, **235**, 377.
- Mushotzky, R. F., Cowie, L. L., Barger, A. J., Arnaud, K. A., 2000, *Nature*, **404**, 459.
- Nandra, K., Pounds, K. A., 1994, *MNRAS*, **268**, 405.
- Nowak, M. A., Vaughan, B. A., Wilms, J. et al., 1999, *ApJ*, **510**, 874.
- Orr M.J.L., Browne I.W.A., 1982, *MNRAS*, 200, 1067
- Osterbrock, D. E., 1989, *Astrophys. of gaseous nebulae and active galactic nuclei*, University Science Books.
- Page, K. L., Reeves, J. N., O'Brien, P. T. & Turner, M. J. L., 2005, *MNRAS*, **364**, 195.
- Peterson, B. M., 1993, *PASP*, **105**, 247.
- Peterson, B. M., 1997, *An introduction to active galactic nuclei*, Cambridge University Press.
- Piccinotti, G. et al., 1982, *ApJ*, **253**, 485.
- Pounds, K. A., Nandra, K., Stewart, G. C., George, I. M., and Fabian, A. C., 1990, *Nature*, **344**, 132.
- Reis, R. C., & Miller, J. M., 2013, *astro-ph.HE*, arXiv:1304.4946v1, 17 April 2013.
- Reynolds, C. S., 2000, *ApJ*, **533**, 811.
- Risaliti, G., Maiolino, R., Salvati, M., 1999, *ApJ*, **522**, 157.
- Risaliti, G. et al., 2013, *Nature*, **494**, 449 .
- Sambruna, R. M., Eracleous, M. & Mushotzky, R. F., 1999, *ApJ*, **526**, 60
- Sato, R., Kataoka, J., Takahashi, T., et al. 2008, *ApJ*, **680**, L9.
- Schaefer, J. et al. 2004, *AGN Physics with Sloan Digital Sky Survey (ASP Conf. Ser. 311)*, ed. G. T. Richards & P. T. Hall (San Francisco, CA: ASP), 329
- Scheuer P.A.G., Readhead A.C.S., 1979, *Nature*, 277, 182

- Shakura, N. I., Sunyaev, R. A., 1973, *A & A.*, **24**, 337.
- Shankar, F., Dai, X., Sivakoff, G. R. 2008, *ApJ*, **687**, 859.
- Sikora, M., Begelman, M. C., Rees, M. J., 1994, *ApJ*, **421**, 153.
- Singh, K. P., Agrawal, P. C., Manchanda, R. K., Naranan, S., & Sreekantan, B. V., 1983, *A&A*, **117**, 319.
- Singh, K. P., Garmire, G.P., and Nousek, J., 1985, *ApJ.*, **297**, 633.
- Singh, K. P., Westergaard, N. J., Schnopper, H.W., 1987, *A & A Letters*, **172** , 11.
- Singh, K. P., Westergaard, N. J., Schnopper, H. W., Awaki, H., and Tawara, Y. 1990, *ApJ.*, **363**, 131.
- Singh, Kulinder Pal, 2005, Techniques in X-ray Astronomy I. Imaging Telescopes, *Resonance*, **10**, No. 6, 15.
- Singh, K. P., 2011, *Journal of Optics*, Vol. 40, Issue 3, 88.
- Takahashi, T., Tashiro, M., Madejski, G., et al. 1996, *ApJ*, **470**, L89.
- Takahashi, T., Kataoka, J., Madejski, G., et al. 2000, *ApJ*, **542**, L105.
- Tanaka, Y., Inoue, H., Holt, S. S., 1994, *Pub. Astron. Soc. Japan*, **46**, L37.
- Tanaka, Y., Nandra, K., Fabian, A. C., et al., 1995, *Nature*, **375**, 659.
- Tavecchio, F., Maraschi, L., Ghisellini, G. et al., 2007, *ApJ*, **665**, 980.
- Tramacere, A., Giommi, P., Perri, M., Verrecchia, F., & Tosti, G. 2009, *A & A*, **501**, 879.
- Turner, T. J. and Pounds, K. A., 1989, *MNRAS*, **240**, 833.
- Urry, M.C. & Padovani, P., 1995, *PASP*, **107**, 803.
- Uttley, P., McHardy, I.M., Papadakis, I. E., 2002, *MNRAS*, **332**, 231.
- Vaughan, B. A. & Nowak, M. A., 1997, *ApJ*, **474**, L43.
- Vaughan, S. & Fabian, A. C., 2004, *MNRAS*, **348**, 1415.
- Voges, W. et al., 1999, *A&A*, **349**, 389.
- Weymann, R. J. & Morris, S. L. 1991, *ApJ*, **373**, 23.
- Wilman, R. J., Fabian, A. C., 1999, *MNRAS*, **309**, 862.
- Wilman, R. J., Fabian, A. C., and Gandhi, P., 2000, *MNRAS*, **318**, L11.
- Worsley, M. A. et al., 2004, *MNRAS*, **352**, L28.
- Yuan, W., Fabian, A. C., Worsley, M. A. & McMahon, R. G., 2006, *MNRAS*, **368**, 985.
- Zakamska, N. L. et al., 2004, *AJ*, **128**, 1002.
- Zoghbi, A., Fabian, A. C., Reynolds, C. S., & Cackett, E. M., 2012, *MNRAS*, **422**, 129.
- Zoghbi, A., Reynolds, C., Cackett, E. M., Miniutti, G., Kara, E., & Fabian, A.C., 2013, *ApJ*, **767**, 121.